Resonance production in $K^-n \to \Sigma^-\pi^+\pi^-(\pi^0)$ reactions at 2.87 GeV/c

E. Katsoufis,* J. Canter,† W. A. Mann, J. Schneps, J. Tompkins,‡ and G. Wolsky§
Tufts University, Medford, Massachusetts 01255

S. A. Gourevitch,‖ L. Kirsch, and P. Schmidt
Brandeis University, Waltham, Massachusetts 02154

(Received 9 January 1978)

A search for exotic $I = 2$ hyperons decaying into $\Sigma^-\pi^-$ or $\Sigma^-\pi^-\pi^0$ has been completed in the final states $\Sigma^-\pi^+\pi^-$ and $\Sigma^-\pi^+\pi^-\pi^0$ produced in K^-n interactions at 2.87 GeV/c. Cross sections for these two final states are 303 ± 31 μb and 660 ± 66 μb, respectively. Upper limits for exotic processes are $\sigma(K^-n \to Y^{*--}\pi^+,\ Y^{*--} \to \Sigma^-\pi^-) < 13$ μb and $\sigma(K^-n \to Y^{*--}\pi^+,\ Y^{*--} \to \Sigma^-\pi^-\pi^0) < 23$ μb for $\Gamma(Y^{*--}) < 120$ MeV; $\sigma(K^-n \to Y^{*--}\pi^+\pi^0,\ Y^{*--} \to \Sigma^-\pi^-) < 28$ μb for $\Gamma(Y^{*--}) < 80$ MeV. Production cross sections have also been measured for all nonexotic resonances observed in the two final states.

I. INTRODUCTION

The color-flavor quark model, in which quarks are bound by an octet of color gluons to form the known hadrons, has achieved considerable favor recently.[1] One of the attractive features of the color aspect of this model is that it provides a natural description of saturation at the quark-antiquark level for mesons and at the three-quark level for baryons.[2] On the other hand, it has been pointed out[3] that two-component duality with factorization requires the existence of exotic hadrons containing $q\bar{q}q\bar{q}$ for mesons and $qqq\,q\bar{q}$ for baryons, and that dual resonance models will not be tenable if such resonances are not found. Rough estimates for the masses suggest that the lowest-lying states should occur below 3 GeV/c^2. It is not certain at this time whether the Z^* enhancements detected in K^+-nucleon interactions are indeed exotic resonances.[4] It is clear that a great deal of experimental work remains to be done before the existence or nonexistence of exotic states can be settled.

It is also clear, if recent phenomenology based upon the bag model is any indication, that resonance hunting in nonexotic final states continues to be of interest. For example, it is suggested that there are $q^4\bar{q}$ hyperons which decay into broad Λ^* and Σ^* channels and appear among signals from q^3 states.[5]

We present a study of the final states $\Sigma^-\pi^+\pi^-$ and $\Sigma^-\pi^+\pi^-\pi^0$ resulting from K^-n interactions with a beam momentum of 2 87 GeV/c, corresponding to 2.57 GeV average energy available in the center of mass. The data were obtained using a 10.2-event/μb portion of a 10^6-picture exposure of the 31 in. deuterium-filled bubble chamber at Brookhaven National Laboratory. An analysis of final states containing two or more visible decays of strange particles obtained from the full exposure has been published.[6] These results included upper limits on production of $I = \frac{3}{2}$ Ξ^{*--} states. In the present experiment a search has been undertaken for $S = -1$, $I = 2$ exotic hyperons having masses <2.4 GeV/c^2 and decaying into $\Sigma^-\pi^-$ or $\Sigma^-\pi^-\pi^0$. In order to obtain reliable upper limits for these states, the production features of all hyperon and vector-meson resonances observed in our $\Sigma^-\pi^+\pi^-(\pi^0)$ final states have been studied. Previous bubble-chamber experiments have explored some features of $\Sigma^-\pi^+\pi^-(\pi^0)$ production in K^-n interactions at 2.11 and 2.65,[7] 3.0,[8] 4.93,[9] and (Ref. 10) 5.5 GeV/c.

II. EXPERIMENTAL PROCEDURES

The film was scanned for three- and four-prong topologies in which one negative track exhibited a kink, a configuration characteristic of both Σ^- and K^- decays. Visible spectator protons were included in the prong count. Templates were used to reject kinking negative tracks with a turning angle $\alpha = 0.3Hc\tau/m$ greater than 8°, where τ is the mean Σ^- lifetime and m is its mass. This restriction allowed selection of Σ's with lifetimes <5.7 Σ^- mean lives while rejecting kaons with lifetimes >0.03 K^- mean lives. Approximately 17 000 events were measured and geometrically reconstructed. The kinematic-fitting program SQUAW was used to make multivertex fits to the hypotheses

$$K^-d \to \Sigma^-\pi^+\pi^-\mathrm{mm}(p_s), \quad (1)$$

$$K^-d \to \Sigma^-\pi^+\pi^-(p_s), \quad (2)$$

$$K^-d \to \Sigma^-\pi^+\pi^-\pi^0(p_s), \quad (3)$$

with the subsequent decay $\Sigma^- \to n\pi^-$. The symbol p_s represents either a measured or an unmeasured spectator proton; mm is a missing mass.

An unseen spectator was assigned momentum components $P_x = P_y = 0 \pm 30$ MeV/c, $P_z = 0 \pm 50$ MeV/c and treated as a measured track. Approximately 70% of the Σ^- tracks were too short to allow measurement of the Σ^- momentum. In such cases the decay fit was a zero-constraint calculation which, for 1% of the candidates for reaction (2) and for 14% of the candidates for reaction (3), resulted in two distinct multivertex fits to the same hypothesis having Σ^- momenta differing by more than 0.04 GeV/c. All events containing kinematic ambiguities of this type were examined by a physicist. In 49% of these events we were able to unambiguously select our solution using the Σ^- ionization. Where this was not possible we have retained both solutions and weighted each by 0.5. Events which fit neither hypothesis (2) nor hypothesis (3) with a χ^2 probability >0.1%, but which nevertheless had a missing mass in hypothesis (1) which was less than the mass of two π^0's, were candidates for remeasurement.

To avoid biases in the event sample arising from scanning or geometrical reconstruction, it was necessary to impose the following additional criteria:

(a) The Σ^- decay length projected onto the film plane was required to be greater than 0.5 cm.

(b) The projected angle between the Σ^- and π^- tracks in the $\Sigma^- \to \pi^- n$ decay was required to be greater than 5°.

(c) A rectangular fiducial volume, extending 73 cm along the incident beam direction, was imposed on Σ^- decay vertices to ensure more than 2.5 cm of projected track length on decay π^- tracks. A more restrictive fiducial volume used for production vertices required that they be more than 1 cm inside the decay fiducial volume.

(d) Only those events with Σ^- lifetimes less than three mean lives were used, in order to further minimize contamination from K^- decays.

Corrections for losses incurred by the above selections have been made using geometrical weighting procedures[11] in which each event is weighted by the inverse of its probability to be found within the cuts. The average geometrical weight is 1.42.

The χ^2 probability distributions for hypotheses (2) and (3), examined separately for events with and without measurable spectator protons, were found to be uniform except for the low probability region. Consequently, all events having a χ^2 probability less than 5% have been removed from our sample, and a correction factor of 1.05 ± 0.02 has been applied to the remaining events.

The proton momentum distribution for the events fitting reaction (2) has been examined. Below a proton momentum of 250 MeV/c the combined distribution of both seen and unseen proton momenta is in agreement with the spectrum expected on the basis of either the Hulthén or the Hamada-Johnston deuteron wave functions.[12] There is, however, an excess of events having proton momentum greater than 250 MeV/c, most probably due to secondary scattering within the target deuterons. We have therefore restricted our final samples of reactions (2) and (3) to events having a spectator momentum less than 250 MeV/c. The production angular distribution of measured spectator protons in this final sample is isotropic. A correction factor of 1.06 ± 0.06 applied to the remaining sample accounts for the loss of events incurred by this selection. This factor has been calculated using a Hamada-Johnston distribution; the assigned error reflects the uncertainty in the model.

After all selection criteria were imposed, 1122 events fit hypothesis (2) and did not fit hypothesis (3), 3160 events fit hypothesis (2), and 157 events (144 of which involve an unseen spectator) had an acceptable fit to both hypotheses. The distributions in $M(\Sigma^-\pi^+)$ and $M(\pi^+\pi^-)$ for the ambiguous events contain structure characteristic of unique $\Sigma^-\pi^+\pi^-$ events [for example, clear evidence of production of $\rho^0(770)$]. Since the $\pi^+\pi^-\pi^0$ invariant-mass spectrum for these same events shows no indication of production of $\omega(783)$, which is prominent in the sample of unambiguous four-body events, the entire ambiguous sample has been assigned to the more highly constrained hypothesis.

A more serious problem, affecting both the three- and four-body final states, is the possibility of background contamination due to kinematic overlap with the reactions

$$K^-d \to \Sigma^-K^+K^-(p_s), \tag{4}$$

$$K^-d \to \Sigma^-K^+K^-\pi^0(p_s). \tag{5}$$

We expect, and have found, this effect to be more substantial for the one-constraint $\Sigma^-\pi^+\pi^-\pi^0$ events than for the four-constraint $\Sigma^-\pi^+\pi^-$ sample. Fits to reactions (4) and (5) were attempted for approximately one third of the $\Sigma^-\pi^+\pi^-$ sample. Only two of these events successfully fit the $\Sigma KK(\pi^0)$ hypotheses, indicating a contamination from these reactions of less than 1% at the 90% confidence level.

Fits to reactions (4) and (5) have been attempted for all events in the $\Sigma^-\pi^+\pi^-\pi^0$ sample. The 197 events which fit the 4C reaction (4) with a χ^2 probability $P(\chi^2) > 1\%$ have been removed from the sample. We note that the distribution in $M(K^+K^-)$ for those events was consistent with the corresponding spectrum observed[6] in the final state $\Sigma^-K^0\overline{K}^0$ at this momentum, which contained approximately 58% $\phi(1019)$ production. An addition-

al 291 events either fit reaction (4) with $P(\chi^2)$ $<1\%$, or fit reaction (5). After examination of the ionization of the meson tracks for these events and of the distributions in $M(K^+K^-)$, an additional 44 events have been removed; our analysis indicates that the remaining sample contains a possible contamination of 36 ± 8 $\Sigma KK(\pi^0)$ events.

Additional sources of background events which we have considered are the reactions $K^-d \to \Sigma^-K^\pm\pi^\mp K^0(p_s)$ with the K^0 decay undetected, and $K^-d \to \Sigma^-\pi^+\pi^- + n\pi^0$ with $n \geq 2$. Cross sections for the former reactions have been measured in an analysis of strangeness -2 states in this exposure.[6] For an unobserved K^0 they are 1.1 ± 0.6 μb for the final state $\Sigma^-K^-\pi^+K^0$ and 1.5 ± 0.7 μb for the final state $\Sigma^-K^+\pi^-\overline{K}^0$, indicating a possible contamination of 11 ± 4 events. We have checked for multi-π^0 production by examining the distribution in (missing mass)^2 from $K^-n \to \Sigma^-\pi^-\pi^+ +$ missing mass. The spectra for both measured and unmeasured spectator protons can be adequately fitted by Gaussian-like distribution functions symmetric about $M_{\pi^0}{}^2$. At the 90% confidence level, there is an excess of not more than 49 events having (missing mass)^2 $>M_{\pi^0}{}^2$.

As a final check on the purity of the $\Sigma^-\pi^-\pi^+\pi^0$ sample, 500 events were examined by physicists for compatibility between the observed ionization of measured tracks and the ionization indicated by the kinematic fit. Twelve events were found to be incompatible with the reaction (3) hypothesis. These events have been removed, and we estimate a remaining contamination of 58 ± 17 events arising from unobserved track scatters, poorly measured tracks, and other misidentified events.

Our final samples, therefore, consist of 1273 $\Sigma^-\pi^+\pi^-$ events and 2907 $\Sigma^-\pi^+\pi^-\pi^0$ events, which after correction for the geometrical detection efficiencies, correspond to weighted event samples of 1814 and 4097, respectively. The contaminations due to competing hypotheses and reconstruction error are $(0.7\pm0.2)\%$ for the $\Sigma^-\pi^+\pi^-$ final state and $(3.6\pm0.7)\%$ for the $\Sigma^-\pi^+\pi^-\pi^0$ final state.

III. CROSS-SECTION DETERMINATIONS

Reaction cross sections have been calculated using the relation

$$\sigma_j = G\sum_{i=1}^{N_j} W_i(j)/(Ln\epsilon),$$

where the sum is over all the N_j events fitting the jth reaction. $W_i(j)$ is the individual event weight reflecting geometric and kinematic selections, L is the total beam path length corrected for interaction and decay, and n is the neutron target number density.[13] The factor $G=1.05\pm0.02$ is the usual Glauber correction[14] which accounts for the partial screening of the neutron by the proton in the deuteron nucleus. The factor ϵ is an overall experimental efficiency which, in addition to weights to account for χ^2 probability and spectator-proton momentum selections, contains corrections for losses of events during scanning and processing. A scanning efficiency of 0.99 was established, using the standard Geiger-Werner method, for a sample of the film (approximately one half of the total) upon which a second scan was performed. As a check on whether losses in scanning were indeed random, a subsample of the doubly scanned film was scanned a third time and the results analyzed using the visibility-dependent Derenzo-Hildebrand technique.[15] That study supports the double-scan efficiency and indicates that a reasonable error is ±0.02.

Only those events found in the film sample which was scanned twice were remeasured and reprocessed if the first measurement failed to yield an acceptable fit to reactions (1)–(3). Losses during reconstruction and fitting have been estimated from failure rates in the first and second measurements of these events. When losses due to unmeasurable events are included, we obtain a processing efficiency of 0.82 ± 0.03 for the twice-scanned, twice-measured film sample.

Although the entire 10.2 events/μb sample has been used in our resonance search, the determination of the reaction cross sections quoted in this paper has been restricted to that portion of the exposure which was scanned and measured twice. This sample has a μb equivalent (Ln) of 5.09 ± 0.23 events/μb and an experimental efficiency $\epsilon=0.73\pm0.05$. We find cross sections of 303 ± 31 μb and 660 ± 66 μb, respectively, for the reactions $K^-n \to \Sigma^-\pi^+\pi^-$ and $K^-n \to \Sigma^-\pi^+\pi^-\pi^0$. These values are in agreement with measurements made by the SABRE collaboration at 3.0 GeV/c, who obtained 340 ± 25 μb and 670 ± 50 μb, respectively, for the same reactions.[16]

IV. THE FINAL STATE $\Sigma^-\pi^+\pi^-$

The Dalitz plot for this final state is shown in Fig. 1. Strong bands in the intervals $0.50 \leq M^2 \leq M^2(\pi^+\pi^-) \leq 0.68$ (GeV/c^2)^2 and $2.25 \leq M^2(\Sigma^-\pi^+) \leq 2.50$ (GeV/c^2)^2, corresponding to production of $\rho^0(770)$ and $\Lambda(1520)$, respectively, are evident. There is also an accumulation of events near the lower edge of $(\Sigma^-\pi^+)$ phase space [$M^2(\Sigma^-\pi^+) < 2.05$ (GeV/c^2)^2]. These structures are displayed more clearly in the invariant-mass projections of Fig. 2.[17] The dashed curves in Figs. 2(a) and 2(c) represent the distributions expected for the following

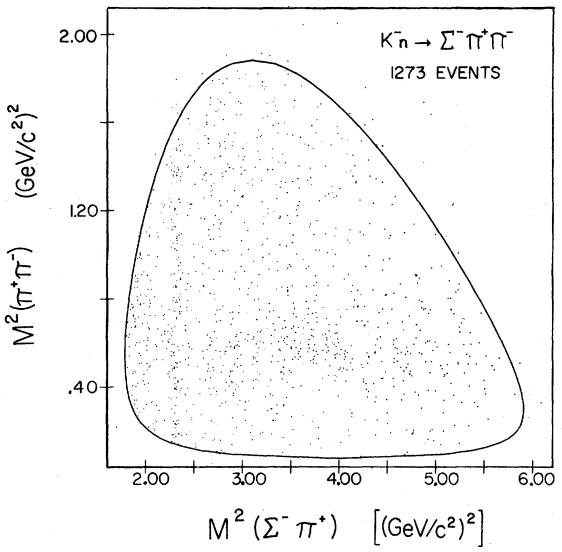

FIG. 1. The $\pi^+\pi^-$ versus $\Sigma^-\pi^+$ Dalitz plot for the final state $\Sigma^-\pi^+\pi^-$.

set of processes:

$K^-n \to \Lambda(1520)\pi^-$ (16%),

$K^-n \to \Sigma^-\rho^0(770)$ (26%),

$K^-n \to \Sigma^-\pi^+\pi^-$ (phase space).

The assumption of only $\Lambda(1520)$ and $\rho^0(770)$ production is clearly inadequate, since in the $\Sigma^-\pi^+$ spectrum there is a clear enhancement in the $\Sigma^0(1385)/\Lambda(1405)$ region ($1.34 < M(\Sigma^-\pi^+) < 1.44$ GeV/c^2), as well as a broad enhancement in the interval $1.60 < M(\Sigma^-\pi^+) < 1.90$ GeV/c^2 suggestive of unresolved Y^* structure. We have been able to separate the several participating signals by an examination of their t dependence. In the Chew-Low plot of Fig. 3, the $\Delta(1520)$ can be seen to be abundantly produced at all allowed t values. In addition, clustering of events at low values of $|t|$ is apparent around $M^2(\Sigma^-\pi^+) = 2.00$ and 3.0 (GeV/c^2)^2. When we select events having $|t| > 0.35$ (GeV/c)^2 we obtain the $\Sigma^-\pi^+$ mass distribution shown in Fig. 4(a). The smooth curve is a Monte Carlo simulation of the distribution expected for $|t| > 0.35$ (GeV/c)^2 when, in addition to phase space, the processes $K^-n \to \Sigma^-\rho^0(770)$ (26.3%), $K^-n \to \Lambda(1405)\pi^-$ (17.4%, and $K^-n \to \Sigma^0(1385)\pi^-$ (4.0%) are present. We have used the empirical four-momentum-transfer distributions for these three signals. The mass enhancements at 1.66 and 1.84 GeV/c^2, which we identify as production of $\Sigma^0(1660)$ and $\Lambda(1830)$, are each approximately three standard deviations above the expected background.

Similarly, Fig. 4(b) contains the corresponding mass distribution and simulated background curve

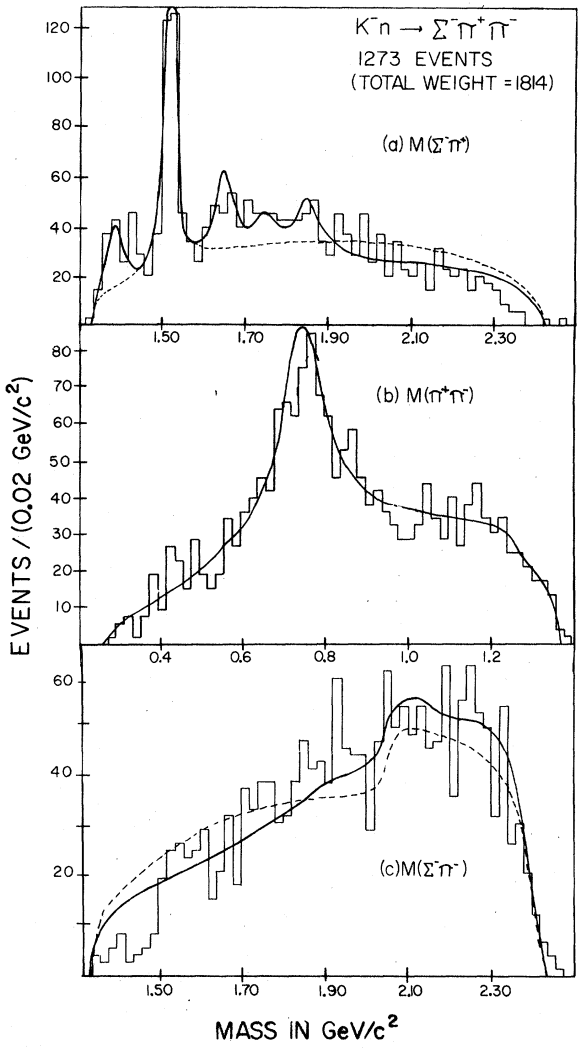

FIG. 2. The invariant-mass distributions for the final state $\Sigma^-\pi^+\pi^-$: (a) $M(\Sigma^-\pi^+)$, (b) $M(\pi^+\pi^-)$, (c) $M(\Sigma^-\pi^-)$. The dashed curves on (a) and (c) represent the distributions which would be expected if only $\Lambda(1520)$ and $\rho^0(770)$ were produced in addition to phase space. The solid curve represents our best fit to the data, and corresponds to the resonance parameters of Table I.

for $|t| < 0.35$ (GeV/c)^2. This yields an enhanced $\Sigma(1385)/\Lambda(1405)$ signal, as well as a smaller peak centered at 1.74 GeV/c^2. The $\Sigma^0(1385)$ signal appears to be divided nearly equally between $|t| > 0.35$ (GeV/c)^2. If the excess of events having $|t| < 0.35$ (GeV/c)^2 and $1.41 \leq M(\Sigma^-\pi^+) < 1.44$ GeV/c^2 is interpreted as $\Lambda(1405)$ production, its appearance only for these low values of $|t|$ is consistent with the very peripheral behavior of this state observed in K^-n interactions at 3.0 GeV/c.[8] We note also that there is no evidence in the data for a $\Sigma(1475)$ reported previously in $(\Lambda\pi^+)K^+$ and $(\Sigma^+\pi^0)K^+$ final

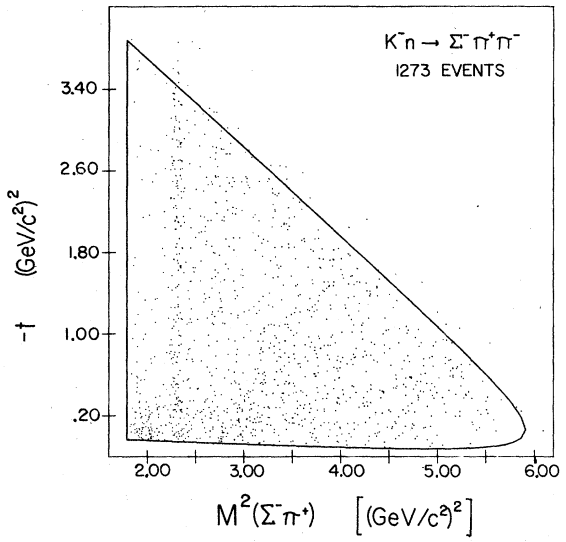

FIG. 3. The Chew-Low plot for the $\Sigma^-\pi^+$ system in the final state $\Sigma^-\pi^+\pi^-$.

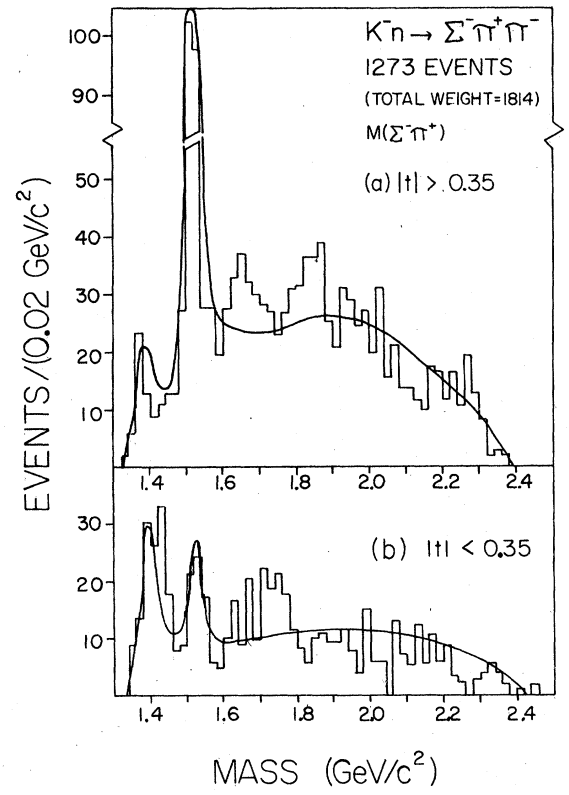

FIG. 4. The distributions in $M(\Sigma^-\pi^+)$ after selections on the four-momentum transfer $|t|$ from the beam K^- to the final state π^- have been applied: (a) $|t| > 0.35$ $(GeV/c)^2$, (b) $|t| < 0.35$ $(GeV/c)^2$. The solid curves represent a Monte Carlo simulation of the distributions expected for $\Sigma^0(1385)$, $\Lambda(1520)$, and $\rho^0(770)$ production plus phase space.

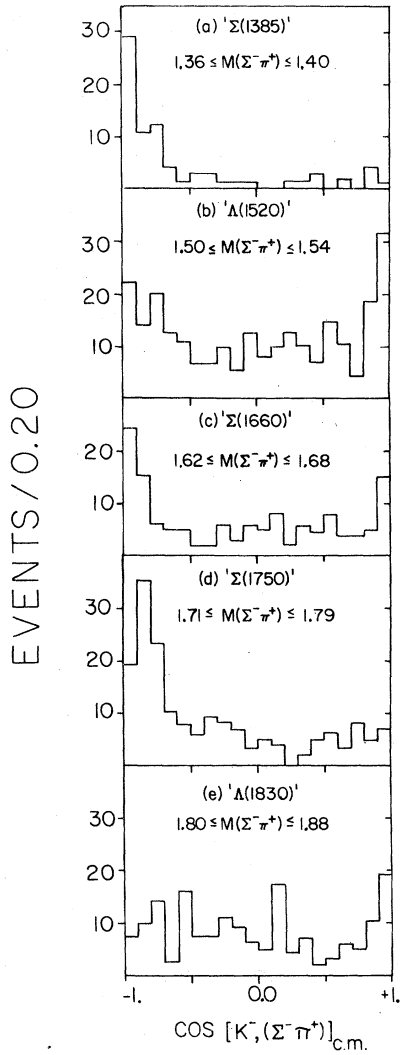

FIG. 5. The center-of-mass production augular distributions ($\hat{K}^- \cdot \hat{Y}^*$) for the five identified resonant signals in the final state $\Sigma^-\pi^+\pi^-$. No background subtraction has been applied to the indicated mass regions.

states produced in 1.7-GeV/c π^+p reactions.[18] The existence of a Σ^* at about this mass, which decays predominantly via the $\Sigma\pi$ mode, is predicted by the quark shell model of Horgan and Dalitz.[19] The mass interval $1.46 \le M(\Sigma^-\pi^+) \le 1.50$ GeV/c^2 yields an upper limit[20] of 3.3 μb at the 90% confidence level for the production of a $\Sigma^0(1475)$ having $\Gamma < 40$ MeV. The signal in the mass interval $1.70 \le M(\Sigma^-\pi^+) \le 1.78$ GeV/c^2, which is approximately 3.0 standard deviations above background, is interpreted as production of $\Sigma^0(1750)$.

Figure 5 contains the center-of-mass production angular distributions for the five mass regions containing the Y^* signals suggested in Figs. 2 and 4. No background subtraction has been attempted.

TABLE I. Fit parameters and partial cross sections for the final state $\Sigma^-\pi^+\pi^-$. Values of masses and widths without quoted error were held constant during the fit. Cross sections are not corrected for alternate decay modes of resonant systems.

Final state	Mass (MeV/c^2)	Width (MeV)	Percentage of final state (%)	Cross section (μb)
$\Sigma^0(1385)\pi^-$	1388 ± 4	53 ± 15	4.0 ± 1.7	12.1 ± 5.3
$\Lambda(1520)\pi^-$	1519 ± 7	25 ± 3	17.4 ± 1.4	52.7 ± 6.9
$\Sigma^0(1660)\pi^-$	1655	60	~8.0[a]	~24
$\Sigma^0(1750)\pi^-$	1750	70	~4.0[a]	~12
$\Lambda(1830)\pi^-$	1850	70	~6.0[a]	~18
$\Sigma^-\rho^0(770)$	750 ± 7	128 ± 20	26.3 ± 2.2	79.7 ± 10.5

[a]These are our best estimates for the fixed masses and widths quoted. These signals are distinguishable in the data only after the four-momentum-transfer selections discussed in the text. Because of the close proximity in invariant mass for these signals $[(m_i - m_j) < (\Gamma_i + \Gamma_j)]$ there is substantial correlation among their parameters, with the consequent possibility of significant systematic error in their relative fractions. We therefore do not quote errors for these quantities.

With the exception of $\Lambda(1830)$, all of the signals exhibit structure in the angular distributions consistent with their interpretation as resonance production. Peripheral peaks, suggesting meson exchange production mechanisms, are evident. In addition, the $\Lambda(1520)$ region contains a strong antiperipheral peak indicating the presence of baryon exchange. This is consistent with similar behavior observed in the process $K^-n \to \Lambda(1520)\pi^-$ at 4.93 and 5.5 GeV/c (Refs. 9 and 10), although the relative baryon exchange contribution appears to be decreasing with increasing beam momentum.

It appears, therefore, that production of $\rho^0(770)$, $\Sigma^0(1385)$, $\Lambda(1520)$, $\Sigma^0(1660)$, $\Sigma^0(1750)$, and $\Lambda(1830)$ all represent non-negligible fractions of the $\Sigma^-\pi^+\pi^-$ final state. We have measured the mass, width, and percentage for the first three states using the maximum-likelihood technique.[21] During the fit, the nominal mass and width of the three higher mass Y^* signals were used, and their amounts allowed to vary. The results are given in Table I, where the fractions for each contributing process are also expressed as cross sections corresponding to the observed decay mode of the resonance involved. Because of the close proximity of these three resonances and the substantial correlation of errors in the mass, widths, and fractions of each, we have chosen to quote only our best estimate for the fractions and widths. Their reflection of the $\Sigma^-\pi^-$ mass spectrum is insensitive to variations in the masses and widths.

The solid curves in Fig. 2 represent this solution. As can be seen in Fig. 2(c), the observed distribution in $M(\Sigma^-\pi^-)$ is reasonably accounted for by reflections of the resonances occurring in the nonexotic $(\Sigma^-\pi^+)$ and $(\pi^+\pi^-)$ systems. There is no significant evidence for production of a Y^{*--} in the data. We have measured upper limits on the production of resonances decaying into $\Sigma^-\pi^-$ by selecting that region of the $\Sigma^-\pi^-$ spectrum containing the greatest number of events above background $(1.82 < M(\Sigma^-\pi^-) < 2.00$ GeV/c^2). At the 90% confidence level we find

$\sigma < 8.6$ μb, $\Gamma < 60$ MeV

$\sigma < 13.3$ μb, $\Gamma < 120$ MeV.

We note, however, that there have been predictions that the lowest-lying exotic baryons occur with masses $\gtrsim 1.9$ GeV/c^2, and exotic hyperons are expected to be more massive by perhaps 0.150 GeV/c^2 per strange quark.[3] We therefore quote the following upper limits with the additional restriction $M(\Sigma^-\pi^-) > 2.0$ GeV/c^2:

$\sigma < 6.9$ μb, $\Gamma < 60$ MeV

$\sigma < 7.7$ μb, $\Gamma < 120$ MeV.

V. THE FINAL STATE $\Sigma^-\pi^+\pi^-\pi^0$

The geometrically weighted invariant-mass spectra for our final $K^-n \to \Sigma^-\pi^+\pi^-\pi^0$ sample are displayed in Figs. 6–9. In order to determine upper limits on the production of exotic Y^{*--} states, we have attempted to construct likelihood functions based upon all signals observed in the nonexotic meson and hyperon mass projections. It is clear from Figs. 6 and 8(a) that production of $\omega(783)$ and $\Lambda(1520)$ occur in a substantial fraction of the events. Also evident in Fig. 6 is a four to five standard deviation enhancement at 0.980 GeV/c^2, and some indication of production of $\eta(549)$. Following the analysis of Barbaro-Galtieri *et al.*,[22]

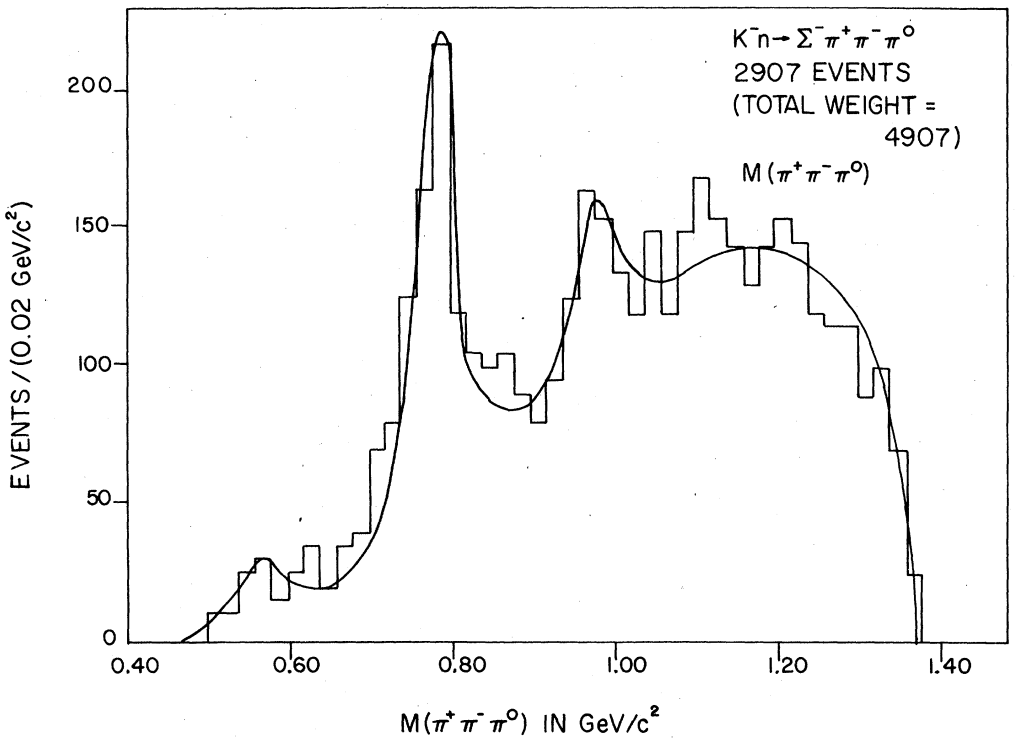

FIG. 6. The invariant-mass distribution $M(\pi^+\pi^-\pi^0)$ for the final state $\Sigma^-\pi^+\pi^-\pi^0$. The solid curve represents a simultaneous maximum-likelihood fit to all mass projections.

we attribute the signal at 0.980 GeV/c^2 to production and decay of $\eta'(958)$ into $\pi^+\pi^-\gamma$, with the decay photon in this process misinterpreted as a π^0 in our fitting procedure. This hypothesis is substantiated when we plot $M(\pi^+\pi^-\gamma')$ for the events having $0.940 \leq M(\pi^+\pi^-\pi^0) \leq 1.020$ GeV/c^2. The result is a sharply peaked distribution, centered at 0.960 GeV/c^2. Also, the distribution in $M(\pi^+\pi^-)$ for this same subsample of events yields a signal corresponding to $\rho^0(770)$ (expected for ~30% of η' decays[18]), which appears as the small enhancement above the fitted curve for $0.680 \leq M(\pi^+\pi^-) \leq 0.800$ GeV/c^2 in Fig. 7(b).

Also evident in Fig. 8(a) are enhancements, above the distributions expected from phase space and the resonances thus far identified, corresponding to production of $\Lambda(1405)$ and $\Sigma^0(1600)$. In the $M(\Sigma^-\pi^0)$ distribution of Fig. 8(b), the relatively weak signal occurring at 2.020 GeV/c^2 has been identified with $\Sigma^-(2030)$ production. Finally, the interval $0.660 \leq M(\pi^-\pi^0) \leq 0.800$ GeV/c^2 in Fig. 7(a) contains an excess of events which, after subtraction of reflections due to the other resonant processes, indicates a substantial occurrence of the process $K^-n \to \Sigma^-\pi^+\rho^-(770)$.

Attempts have been made to simultaneously fit all the mass projections using a phase-space distribution plus Breit-Wigner frequency functions for the eight resonance-production processes identified thus far: $K^-n \to \Sigma^-\eta(549)$, $\Sigma^-\omega(783)$, $\Sigma^-\eta'(960)$, $\Sigma^-\pi^+\rho^-(770)$, $\Lambda(1405)\pi^-\pi^0$, $\Lambda(1520)\pi^-\pi^0$, $\Sigma^0(1660)\pi^-\pi^0$, and $\Sigma^-(2030)\pi^+\pi^-$. With the exception of the distributions in $M(\Sigma^-\pi^0)$ [Fig. 8(b)] and $M(\Sigma^-\pi^+\pi^-)$ [Fig. 8(c)], the fitted curves for this solution do not differ significantly from the solid curves shown on the mass projections, which reasonably describe the observed spectra. The dashed curves in Figs. 8(b) and 8(c), however, which represent this eight-resonance fit, strongly suggest that additional resonance structure corresponding to the decay processes $Y^{*-} \to \Sigma^-\pi^0$ and $Y^{*-} \to \Sigma^-\pi^+\pi^-$ are required. In particular, excesses of events near 1.66 and 1.88 GeV/c^2 in $M(\Sigma^-\pi^0)$, and at 1.88 and 2.02 GeV/c^2 in $M(\Sigma^-\pi^+\pi^-)$, suggest the possibility of additional resonant activity in these regions. We note that there are other nonexotic mass projections which contain multibin deviations from the fitted curves of up to three standard deviation significance [e.g., at $M(\pi^-\pi^0) \cong 0.450$ GeV/c^2, $M(\pi^+\pi^-) \cong 0.370$ GeV/c^2, and $M(\pi^+\pi^0) \cong 0.570$ GeV/c^2], but they occur at mass values and in combinations where there has been no evidence for resonances. On the other hand, evidence has been reported[18] for possible

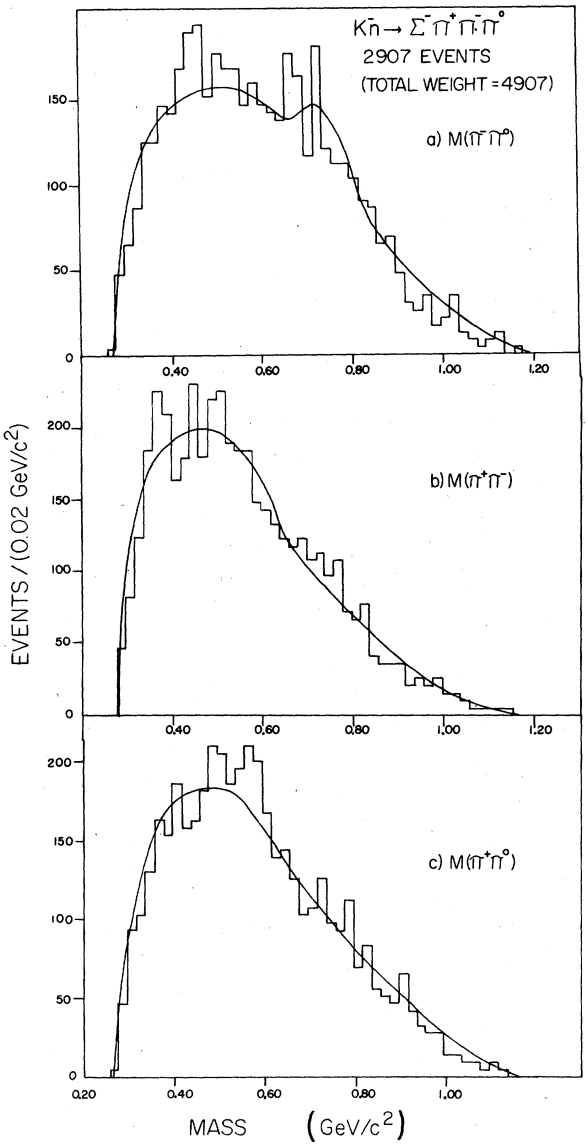

FIG. 7. The dipion invariant-mass distributions for the final state $\Sigma^- \pi^+ \pi^- \pi^0$: (a) $M(\pi^- \pi^0)$, (b) $M(\pi^+ \pi^-)$, (c) $M(\pi^+ \pi^0)$. The solid curves represent a simultaneous maximum-likelihood fit to all mass projections.

Y^* resonant activity near masses of 1.64 and 1.88 GeV/c^2. For this reason, we have added processes involving production and decay of $\Sigma^-(1640)$ and $\Sigma^-(1880)$ into $\Sigma^- \pi^0$, and of $\Sigma^-(1880)$ and $\Sigma^-(2030)$ into $\Sigma^- \pi^+ \pi^-$, to the production and decay sequences previously identified.

The results of fitting using this expanded frequency distribution are presented in Table II, and are represented by the solid curves on the mass projections. With the exception of the depletion of events in the mass interval $2.22 \leq M(\Sigma^- \pi^+ \pi^-)$

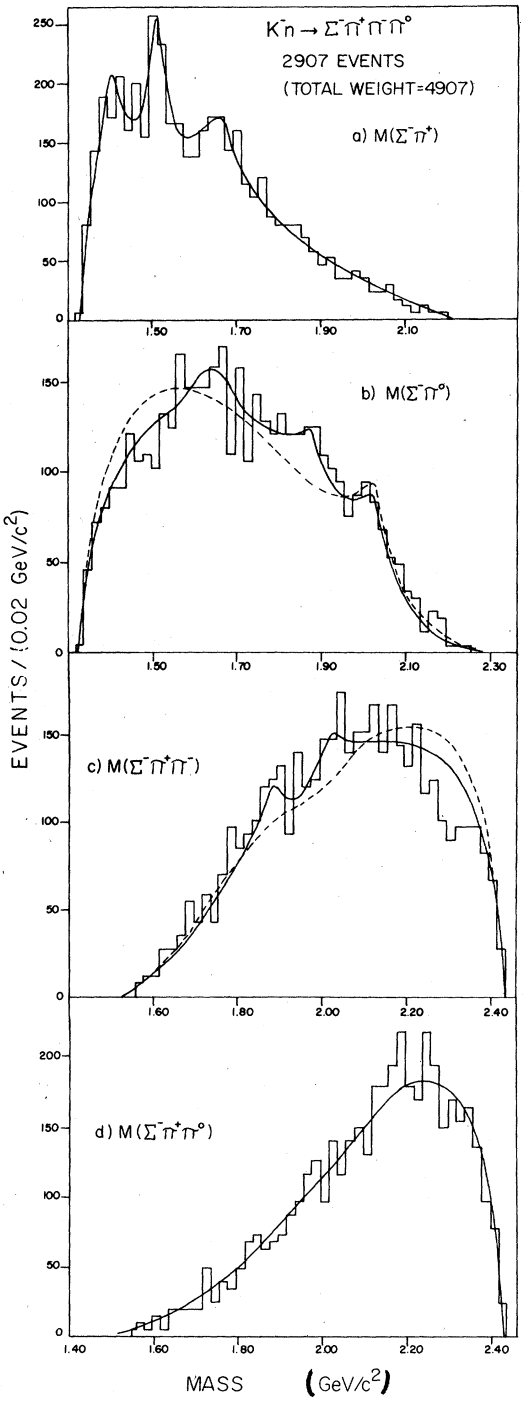

FIG. 8. The nonexotic $\Sigma\pi(\pi)$ mass projections for the final state $\Sigma^- \pi^+ \pi^- \pi^0$: (a) $M(\Sigma^- \pi^+)$, (b) $M(\Sigma^- \pi^0)$, (c) $M(\Sigma^- \pi^+ \pi^-)$, (d) $M(\Sigma^- \pi^+ \pi^0)$. The dashed curves in (b) and (c) represent a maximum-likelihood fit to the data involving a minimum number of contributing resonant processes (see text). The solid curves are the final fit involving additional resonant structure at 1.66 and 1.88 GeV/c^2 in $M(\Sigma^- \pi^0)$ and $M(\Sigma^- \pi^+ \pi^-)$.

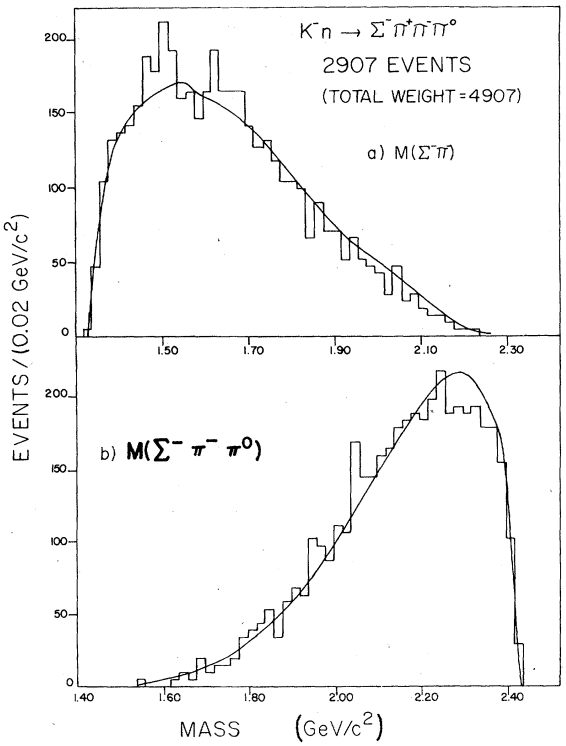

FIG. 9. The invariant-mass distributions for the $Q=-2$ combinations $\Sigma^-\pi^-$ and $\Sigma^-\pi^-\pi^0$ in the final state $\Sigma^-\pi^+\pi^-\pi^0$: (a) $M(\Sigma^-\pi^-)$, (b) $M(\Sigma^-\pi^-\pi^0)$. The solid curves represent the best fit to the data for the production processes listed in Table II.

≤ 2.38 GeV/c^2 [Fig. 8(c)], the distributions in $M(\Sigma^-\pi^0)$ and $M(\Sigma^-\pi^+\pi^-)$ are now acceptably represented. No significant change is made to the other mass spectra, and the goodness of the fit, as measured by the ratio of the χ^2 to the number of constraints, is adequate. Table II also contains our best estimates of the partial cross sections for the twelve resonance production processes indicated by the data. Where comparative data are available [specifically, for the reactions $K^-n \to \Sigma^-\omega(783)$, $\Lambda(1520)\pi^-\pi^0$, $\Sigma^-\pi^+\rho^-(770)$, and $\Sigma^-\eta'(960)$] our measured cross sections agree at the one-standard-deviation level with the results of previous experiments.

We now consider the exotic mass distributions shown in Figs. 9(a) and 9(b), and the interesting question of production and decay of Y^{*--} into $\Sigma^-\pi^-$ and $\Sigma^-\pi^-\pi^0$, respectively. As is clear from Fig. 9(b), we see no evidence for the existence of a Y^{*--} in $M(\Sigma^-\pi^-\pi^0)$. The observed spectrum is well represented by the frequency distribution determined by the nonexotic mass combinations. At the 90% confidence level we obtain the following upper limits on the cross section for the process $K^-n \to Y^{*--}\pi^+, Y^{*--} \to \Sigma^-\pi^-\pi^0$:

$$\sigma < 17\,\mu\text{b}, \quad \Gamma < 60 \text{ MeV}$$

$$\sigma < 23\,\mu\text{b}, \quad \Gamma < 120 \text{ MeV}.$$

The distribution in $M(\Sigma^-\pi^-)$, however, contains a 115-event excess (geometrically weighted) above the fitted distribution in the four bins between 1.46 and 1.54 GeV/c^2. This region contains a total of 693 events, and the statistical significance of the effect is no less than four standard deviations. The cross section corresponding to these events is estimated to be (19.3 ± 4.6) μb. At the 90% confidence level, this data indicates that the cross section for production of a $Y^{*--}(1500)$ with a width $\Gamma < 80$ MeV does not exceed 20 μb. It would ap-

TABLE II. Fit parameters and partial cross sections for the final state $\Sigma^-\pi^+\pi^-\pi^0$. All masses and widths were held constant during the final fit. Cross sections are not corrected for alternate decay modes of resonant systems.

Final state	Mass (MeV/c^2)	Width (MeV)	Percentage of final state (%)	Cross section (μb)
$\Lambda(1405)\pi^-\pi^0$	1405	55	7.2 ± 1.0	47.5 ± 8.1
$\Lambda(1520)\pi^-\pi^0$	1518	35	6.0 ± 0.9	39.6 ± 7.1
$\Sigma^0(1660)\pi^-\pi^0$	1670	60	4.2 ± 1.1	27.7 ± 7.8
$\Sigma^-(1640)\pi^+\pi^-$	1640	100	4.3 ± 1.5	28.4 ± 10.3
$\Sigma^-(1880)\pi^+\pi^-$	1880	80	3.5 ± 1.1	23.1 ± 7.6
$\Sigma^-(1880)\pi^0$	1880	80	3.0 ± 1.4	19.8 ± 9.5
$\Sigma^-(2030)\pi^+\pi^-$	2030	80	6.6 ± 1.5	43.6 ± 10.8
$\Sigma^-(2030)\pi^0$	2030	80	3.6 ± 1.5	23.8 ± 10.2
$\Sigma^-\eta(549)$	549	60	3.4 ± 0.7	22.4 ± 5.1
$\Sigma^-\omega(783)$	783	50	17.5 ± 0.5	115.5 ± 12.0
$\Sigma^-\eta'(960)$	980	60	6.3 ± 1.1	41.6 ± 8.4
$\Sigma^-\rho^-(770)\pi^+$	750	130	11.9 ± 1.5	78.5 ± 12.6

pear that this last statement is the strongest allowed when all the data from this experiment are considered. We note that although we have made every attempt to fit the structure observed in the nonexotic mass distributions using established (and some not-so-well established) resonant systems, there still remain in the data other fluctuations from the fitted distributions which are at or near the statistical level of significance of the effect in $M(\Sigma^-\pi^-)$. No combination of the processes listed in Table II has been found which will significantly alter this situation.

VI. CONCLUSIONS

We have completed a search for evidence of production of exotic Y^{*--} systems in $\Sigma^-\pi^+\pi^-(\pi^0)$ final states produced in K^-n interactions at 2.87 GeV/c. The experiment had a sensitivity of 10.2 events/μb, and spanned the Y^{*--} mass range from 1.34 to 2.5 GeV/c^2. Here, as was the case for strangeness (−2) Ξ^{*--} combinations obtained from the same exposure,[6] we see no statistically significant evidence for any of the following processes:

$$K^-n \to Y^{*--}\pi^+ \to (\Sigma^-\pi^-)\pi^+, \tag{6}$$

$$K^-n \to Y^{*--}\pi^+\pi^0 \to (\Sigma^-\pi^-)\pi^+\pi^0, \tag{7}$$

$$K^-n \to Y^{*--}\pi^+ \to (\Sigma^-\pi^-\pi^0)\pi^+. \tag{8}$$

For Y^{*--} masses above 2.0 GeV/c^2, which from theoretical considerations is the most interesting region, we have measured the following upper limits for the processes (6) and (8), respectively:

$$\sigma < 6.7\ \mu\text{b for } \Gamma(Y^{*--}) < 120\ \text{MeV}, \tag{6'}$$

$$\sigma < 23\ \mu\text{b for } \Gamma(Y^{*--}) < 120\ \text{MeV}. \tag{8'}$$

The distribution $M(\Sigma^-\pi^-)$ from the final state $\Sigma^-\pi^+\pi^-\pi^0$ exhibits a greater than 3-standard-deviation excess in the interval $1.46 \leq M(\Sigma^-\pi^-) \leq 1.54$ GeV/c^2, which would correspond to a Y^{*--} cross section of (19.3 ± 4.6) μb. However, fluctuations of equal or greater magnitude occur in other mass projections for this final state, and we quote only an upper limit of 28 μb at the 90% confidence level for reaction (7).

The mass distributions in the nonexotic hyperon combinations $\Sigma^-\pi^+$, $\Sigma^-\pi^0$, and $\Sigma^-\pi^+\pi^0$ indicate that the two reactions considered here proceed by production of a rich mixture of known or previously suggested resonant systems. Although the statistical significance of most of these signals is marginal, we have estimated their contributions and measured their production cross sections using the maximum likelihood technique. The results are contained in Tables I and II.

Finally we note that the meson systems $\pi^+\pi^-$ and $\pi^+\pi^-\pi^0$ have provided abundant samples of the quasi-two-body reactions,

$$K^-n \to \Sigma^-\rho^0(770) \tag{9}$$

and

$$K^-n \to \Sigma^-\omega(783). \tag{10}$$

Combined with the reaction

$$K^-n \to \Sigma^-\phi(1019) \to \Sigma^-K_S^0 K_L^0, \tag{11}$$

which has been observed[6] to occur in 58% of $\Sigma^-K^0\bar{K}^0$ final states at this energy, they allow the study of production and decay characteristics of vector mesons in the reactions $K^-n \to \Sigma^-V^0$. An analysis will be presented in a subsequent paper.[23]

ACKNOWLEDGMENTS

This work was supported by the Department of Energy. We would like to thank the members of the alternating gradient synchrotron and 31-in bubble chamber staffs of Brookhaven National Laboratory. We also gratefully acknowledge the dilligent efforts of the scanning, technical, and secretarial personnel at Brandeis and Tufts Universities.

*Present address: National Technical University, Athens, Greece.
†Present address: Polariod Corporation, Lexington, Ma 02173.
‡Present address: M. I. T. Lincoln Laboratories, Lexington, Ma 02173.
§Present address: Digital Equipment Corporation, Maynard, Ma 01754.
||Present address: Massachusetts Institute of Technology, Cambridge, Ma 01239.

[1]A. De Rújula, H. Georgi, and S. L. Glashow, Phys. Rev. D 12, 147 (1975).
[2]O. W. Greenberg and D. Zwanziger, Phys. Rev. 150, 1173 (1966); H. J. Lipkin, Phys. Lett. 45B, 267 (1973).
[3]P. G. O. Freund, in *Baryon Resonances*—73, edited by E. C. Fowler (Purdue, West Lafayette, Indiana, 1973), p. 121.
[4]See, for example, Ref. 3, p. 157.
[5]R. L. Jaffe, Phys. Rev. D 15, 267 (1977); D 15, 281 (1977).
[6]E. Briefel, S. A. Gourevitch, L. Kirsch, P. Schmidt, C. Y. Chang, R. Staab, G. B. Yodh, R. Fernow, P. Gauthier, G. Moneti, M. Goldberg, J. Canter, W. A. Mann, J. Schneps, J. Tompkins, and G. Wolsky, Phys. Rev. D 12, 1859 (1975).
[7]A. Barbaro-Galtieri, M. J. Matison, A. Rittenberg, G. B. Chadwick, Z. G. T. Guiragossian and E. Pickup, Phys. Rev. Lett. 21, 573 (1968).

[8]D. Merrill, R. Barloutaud, Duong Nhu Hoa, J. C. Scheuer, A. Verglas, A. M. Bakker, A. J. de Groot, W. Hoogland, J. C. Kluyver, A. G. Tenner, S. A. deWit, S. Focardi, G. Giacomelli, A. Minguzzi-Ranzi, L. Monari, A. M. Rossi, P. Serra, B. Haber, A. Shapira, G. Alexander, Y. Eisenberg, E. Hirsch, G. Yekutieli, U. Karshon, J. Goldberg, E. Huffer, M. Laloum, G. Lamidey, and A. Rouge, Nucl. Phys. B18, 403 (1970); R. Barloutaud, D. Merrill, J. C. Scheuer, A. M. Bakker, W. Hoogland, S. Focardi, A. Minguzzi-Ranzi, A. M. Rossi, B. Haber, U. Karshon, J. Goldberg, G. Lamidey, and A. Rouge, *ibid.* B26, 557 (1971); J. C. Scheuer, R. Barloutaud, D. Merrill, A. M. Bakker, A. J. de Groot, W. Hoogland, G. G. G. Massaro, G. Giacomelli, P. Lugaresi-Serra, A. Minguzzi-Ranzi, A. M. Rossi, G. Alexander, Y. Eisenberg, U. Karshon, A. Shapira, J. Goldberg, G. Lamidey, and A. Rouge, *ibid.* B33, 61 (1971).

[9]F. A. DiBianca, M. B. Einschlag, R. Endorf, A. Engler, H. E. Fisk, and R. W. Kraemer, Nucl. Phys. B35, 13 (1971).

[10]W. Kropac, R. Ammar, R. Davis, H. Yarger, B. Werner, Y. Cho, M. Derrick, D. Johnson, B. Musgrave, T. Wangler, and N. S. Wong, Phys. Rev. D 7, 585 (1973).

[11]R. J. Hemingway and H. Whiteside, University of Maryland Technical Report No. 70-065, 1969 (unpublished); J. Tompkins, Tufts University Bubble-Chamber Group Report No. 9-10, 1973 (unpublished).

[12]L. Hulthén and M. Sugawara, in *Handbuch der Physik*, edited by S. Flugge (Springer, Berlin, 1957), Vol. 39, p. 1; T. Hamada and I. Johnston, Nucl. Phys. 34, 382 (1962).

[13]Details concerning beam purity and target composition are given in Ref. 6.

[14]R. Glauber, Phys. Rev. 100, 242 (1955).

[15]S. Derenzo and R. Hildebrand, Nucl. Instrum. Methods 69, 287 (1969).

[16]D. Merrill *et al.* (Ref. 8), p. 419.

[17]We use weighted events in plotting these and all subsequent invariant-mass distributions.

[18]Yu-Li Pan and F. L. Forman, Phys. Rev. Lett. 23, 806 (1969); 23, 808 (1969).

[19]R. Horgan, Nucl. Phys. B71, 514 (1974); R. Horgan and R. H. Dalitz, *ibid.* B66, 135 (1973).

[20]Our upper limits have been calculated in the following way: A resonance is presumed to exist within the selected mass interval. The resonant "signal" consists of the observed number of events in excess of a background determined by phase space plus the reflections of any identifiable resonances. By assuming that the observed signal is the result of a 1.65-standard-deviation downward fluctuation from a larger number of expected resonant events, an upper limit at the 90% confidence level is obtained.

[21]Maximum-likelihood fitting was accomplished using the program MURTLEBERT. For a description of the method, see J. Friedman, Alvarez Group Programing Note No. P.156, 1966 (unpublished).

[22]A. Barbaro-Galtieri *et al.* (Ref. 7), p. 574.

[23]J. Tompkins, Tufts University Physics Report No. TUFTSPUB-77-1605, 1977 (unpublished).